

C–H Bond Activation of Methane with Gaseous $[(\text{CH}_3)\text{Pt}(\text{L})]^+$ Complexes (L = Pyridine, Bipyridine, and Phenanthroline)

Burkhard Butschke^a, Maria Schlangen^a, Helmut Schwarz^a, and Detlef Schröder^b

^a Institut für Chemie der Technischen Universität Berlin, Straße des 17. Juni 135, 10623 Berlin, Germany

^b Institute of Organic Chemistry and Biochemistry, Flemingovo nám. 2, 16610 Prague 6, Czech Republic

Reprint requests to Dr. D. Schröder. E-mail: Detlef.Schroeder@uochb.cas.cz

Z. Naturforsch. **2007**, *62b*, 309–313; received November 11, 2006

Dedicated to Prof. Helgard G. Raubenheimer on the occasion of his 65th birthday

Electrospray ionization of solutions of dimethyl(1,5-cyclooctadiene)platinum(II) in methanol with traces of nitrogen-containing ligands L provides gaseous complexes of the type $[(\text{CH}_3)\text{Pt}(\text{L})]^+$ with L = pyridine (py), 2,2'-bipyridine (bipy), and 1,10-phenanthroline (phen). These $[(\text{CH}_3)\text{Pt}(\text{L})]^+$ cations are capable of activating the C–H bond in methane as shown by H/D exchange when using CD_4 as a neutral reactant. Most reactive is the complex $[(\text{CH}_3)\text{Pt}(\text{py})]^+$ bearing a monodentate nitrogen ligand. The cationic complexes $[(\text{CH}_3)\text{Pt}(\text{bipy})]^+$ and $[(\text{CH}_3)\text{Pt}(\text{phen})]^+$ also bring about activation of methane, though at a lower rate, whereas the bipyridine complex $[(\text{CH}_3)\text{Pt}(\text{py})_2]^+$ does not react with methane at thermal conditions. A detailed analysis of the experimental data by means of kinetic modeling provides insight into the underlying mechanistic steps, but a distinction whether the reaction occurs as σ bond metathesis or *via* an oxidative addition cannot be made on the basis of the experimental data available.

Key words: C–H Bond Activation, Electrospray Ionization, Mass Spectrometry, Methane, Platinum

Introduction

The activation of methane at ambient conditions has been referred to as one of the “holy grails” in catalysis, and model systems which provide examples for thermal reactions occurring with methane are therefore of paramount interest. Ever since the introduction of the seminal Shilov systems [1], platinum has served as a particularly promising metal for the activation of methane at low temperatures, even though the known procedures are still far from practical applications in large-scale processes [2, 3].

While solution phase experiments have brought a wealth of knowledge about the activation of methane by transition metal complexes [4], gas phase experiments can provide a helpful complement to these approaches in revealing the details of the elementary steps involved in the activation of methane [5]. Particularly intriguing in this respect is a recent debate about the relevance of gas phase studies for reactions occurring in condensed media [6, 7], which dealt with the C–H bond activation of benzene by cationic $[(\text{CH}_3)\text{Pt}(\text{L})]^+$ complexes [8, 9], where L corresponds to a

bidentate nitrogen ligand. Here, we describe the reactions of methane with similar $[(\text{CH}_3)\text{Pt}(\text{L})]^+$ species in the gas phase which are generated directly from solution by means of electrospray mass spectrometry [10].

Methods

The experiments were performed using a VG BIO-Q mass spectrometer which has been described elsewhere [11]. Briefly, the VG BIO-Q is a commercial instrument, which consists of an electrospray ionization (ESI) source combined with a tandem mass spectrometer of QHQ configuration (Q stands for quadrupole and H for hexapole). In the present experiments, mmolar solutions of dimethyl(1,5-cyclooctadiene)platinum(II) and the desired nitrogen ligand L in pure methanol were introduced through a fused-silica capillary to the ESI source *via* a syringe pump (*ca.* 5 $\mu\text{L}/\text{min}$); L = pyridine, 2,2'-bipyridine, and 1,10-phenanthroline. Nitrogen was used as nebulizing and drying gas at a source temperature of 80 °C. Maximal yields of the desired $[(\text{CH}_3)\text{Pt}(\text{L})]^+$ ions were achieved by adjusting the cone voltage in the range of 30 to 60 V. The iden-

tity of the $[(\text{CH}_3)\text{Pt}(\text{L})]^+$ complexes of interest was confirmed by comparison with the expected isotope pattern [12] and collision-induced dissociation (CID). The isotope patterns also assisted in the choice of the adequate precursor ion in order to avoid coincidental mass overlaps of isobaric species in the mass-selected ion beam; accordingly, signals containing either ^{194}Pt , ^{195}Pt , or ^{196}Pt isotopes were chosen for the various ligands [13, 14]. For CID, the ions of interest were mass-selected using Q1, interacted with xenon as a collision gas in the hexapole H under single-collision conditions (typically $2 \cdot 10^{-4}$ mbar) at variable collision energies ($E_{\text{lab}} = 0 - 20$ eV), while scanning Q2 to monitor the ionic products. The reactivity studies described below were performed at a collision energy adjusted to nominally 0 eV at gas pressures ranging from $1 \cdot 10^{-4}$ to $4 \cdot 10^{-4}$ mbar. In several instances, we already have demonstrated that thermal reactions can be monitored under these conditions [15–19], also including gas phase reactions of platinum-containing cations generated *via* electrospray ionization [13].

Results and Discussion

Electrospray ionization of $[(\text{CH}_3)_2\text{Pt}(\text{COD})]$ dissolved in methanol *inter alia* provides access to the monocationic fragment $[(\text{CH}_3)\text{Pt}(\text{COD})]^+$ (COD = 1,5-cyclooctadiene). In the presence of an additional nitrogen ligand in the methanolic solution, *i.e.* L = pyridine (py), 2,2'-bipyridine (bipy), or 1,10-phenanthroline (phen), the COD undergoes partial replacement, thereby offering a simple route for the generation of gaseous $[(\text{CH}_3)\text{Pt}(\text{L})]^+$ complexes. When using the monodentate pyridine as a ligand, also the bis-ligand complex $[(\text{CH}_3)\text{Pt}(\text{py})_2]^+$ is formed in appreciable amounts under ESI conditions. The CID spectra of the mass-selected $[(\text{CH}_3)\text{Pt}(\text{L})]^+$ ions are dominated by losses of the nitrogen ligand L as well as an expulsion of methane; as a minor fragment, the protonated base LH^+ is observed. These results are consistent with the anticipated ion structures and therefore not discussed in any further detail. The purpose of the present experiments was the investigation of the reactions of these ions with methane, where the fully deuterated compound CD_4 is used as a neutral reagent in order to allow a distinction with regard to the methyl group present in the mass-selected $[(\text{CH}_3)\text{Pt}(\text{L})]^+$ complexes of interest.

Of the complexes investigated, namely $[(\text{CH}_3)\text{Pt}(\text{py})]^+$, $[(\text{CH}_3)\text{Pt}(\text{py})_2]^+$, $[(\text{CH}_3)\text{Pt}(\text{bipy})]^+$, $[(\text{CH}_3)\text{Pt}(\text{phen})]^+$, as well as the $[(\text{CH}_3)\text{Pt}(\text{COD})]^+$ ion gen-

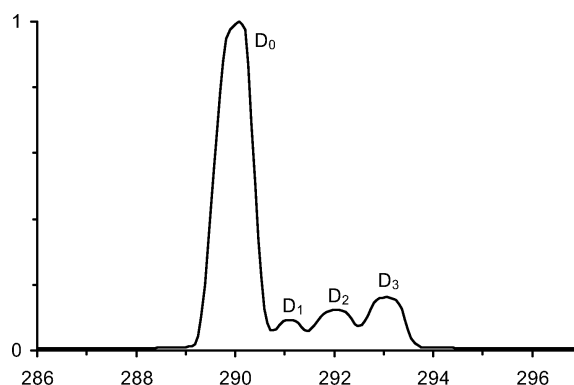


Fig. 1. H/D-Exchange products ($\text{D}_1 - \text{D}_3$) formed in the reaction of mass-selected $[(\text{CH}_3)^{196}\text{Pt}(\text{py})]^+$ (denoted as D_0) with CD_4 at a methane pressure of $3.2 \cdot 10^{-4}$ mbar and a collision energy nominally set to 0 eV.

erated from the platinum precursor compound directly, the species $[(\text{CH}_3)\text{Pt}(\text{py})_2]^+$ and $[(\text{CH}_3)\text{Pt}(\text{COD})]^+$ do not react with CD_4 at a measurable rate, whereas the other ions undergo H/D exchange reactions in the presence of deuterated methane. As an example, the reaction of mass-selected $[(\text{CH}_3)^{196}\text{Pt}(\text{py})]^+$ is shown in Fig. 1, where the precursor ion experiences sequential deuterium incorporation to yield the corresponding complexes with one, two, or three ($\text{D}_1 - \text{D}_3$) deuterium atoms. Even at further elevated CD_4 pressures, neither any exchanges beyond D_3 nor formation of significant amounts of adducts are observed. Accordingly, it is concluded that the coordinated methyl group is in equilibrium with the methane used as a reagent gas, and hence these experiments unambiguously demonstrate the occurrence of C–D bond activation by the monocationic platinum complexes $[(\text{CH}_3)\text{Pt}(\text{py})]^+$, $[(\text{CH}_3)\text{Pt}(\text{bipy})]^+$, and $[(\text{CH}_3)\text{Pt}(\text{phen})]^+$.

For a more detailed analysis of the exchange kinetics, the pressure dependence of the reactions was studied in order to evaluate thermal rate constants as well as accurate branching ratios [20]. Note that consideration of the pressure dependence is particularly important in the case of a degenerate isotope exchange as studied here, because CD_4 is leaked into the hexapole reaction cell at a constant pressure, whereas any $\text{CH}_n\text{D}_{4-n}$ isotopologs ($n = 1 - 3$) formed in the reaction with the $[(\text{CH}_3)\text{Pt}(\text{L})]^+$ complexes are rapidly pumped away. Accordingly, the intensity of the D_3 signal proportionally rises with pressure at the expense of that of the D_1 and D_2 signals (Table 1).

Upon inspection of the data in Table 1, three conclusions immediately become obvious. (i) The iso-

Table 1. Conversion X of the reactant ion^a and isotope patterns of the D_1 , D_2 , and D_3 products^b observed in the thermal ion/molecule reactions of mass-selected $[(CH_3)Pt(L)]^+$ ions with CD_4 at various pressures^c.

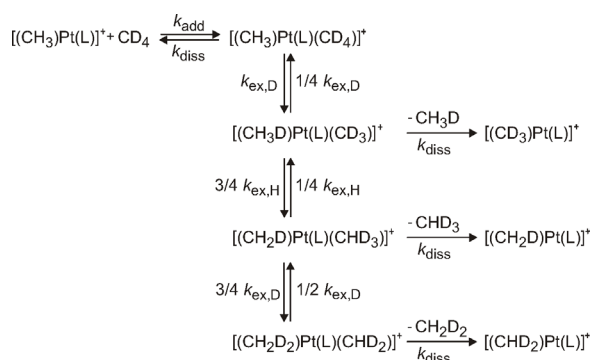
Precursor ion	$p(CD_4)^c$	X^a	D_1	D_2	D_3
$[(CH_3)Pt(py)]^+$	1.5	0.18	28	36	36
	2.2	0.27	24	32	44
	3.2	0.36	20	26	54
$[(CH_3)Pt(bipy)]^+$	1.3	0.04	34	42	24
	2.1	0.05	35	39	26
	2.9	0.06	33	39	28
$[(CH_3)Pt(phen)]^+$	1.8	0.04	34	35	31
	2.9	0.06	32	35	33
	3.9	0.10	33	33	34

a) Conversion X of the parent ion M^+ defined as $X(M^+) = 1 - (I(M^+)/\Sigma I_i)$, where I stands for the ion abundances; b) branching ratios of the D_1 , D_2 , and D_3 ions normalized to $\Sigma = 100$; c) given in 10^{-4} mbar.

tope patterns discount a dominance of specific exchange processes only involving a single H(D) atom, because the D_3 product would prevail largely in this case. (ii) Likewise, product formation does not occur only after complete equilibration of all H and D atoms, for which statistics predict a ratio of 35 : 53 : 12 for the D_1 , D_2 , and D_3 product ions, respectively; here, the D_0 product is ignored because it coincides with the reactant ion. (iii) The pressure dependence of the product-ion ratios is obvious and thus requires an extrapolation of the data to the initial branching ratios of the H/D exchange reaction.

In many cases, isotope patterns obtained in such mass spectrometric measurements can be analyzed by means of reasonable approximations, in which some parameters are neglected or treated only phenomenologically. In the present case, however, such approximations cannot be made because the relevant kinetic parameters, *i. e.* the rate of H/D exchange and the rate of product formation appear to exhibit a similar order of magnitude. In order to derive the kinetic parameters of the underlying elementary steps, an explicit kinetic modeling was performed [21–24].

To this end, let us consider a plausible mechanistic scenario, which consists of the following steps (Scheme 1): (i) Addition of neutral CD_4 to the reactant $[(CH_3)Pt(L)]^+$ leads to the corresponding encounter complex $[(CH_3)Pt(L)(CD_4)]^+$ with the rate constant k_{add} . This intermediate can then either re-dissociate into the reactants (k_{diss}), or undergo C–D bond activation of methane concomitant with C–D bond formation of the methyl carbon atom to afford the isotopologous species $[(CH_3D)Pt(L)(CD_3)]^+$, in which a first H/D exchange within the complex is accomplished (k_{ex}). It is



Scheme 1. Elementary steps for the H/D exchange between $[(CH_3)Pt(L)]^+$ and CD_4 showing the associated rate constants considered in the kinetic modeling.

important to note, however, that dissociation of this particular intermediate leads to the fully deuterated product ion $[(CD_3)Pt(L)]^+$, even though only a single deuterium migration has occurred. In competition with dissociation, the complex $[(CH_3D)Pt(L)(CD_3)]^+$ may also undergo further exchange reactions, for which the rate constants are weighted according to the number of H and D atoms available in the respective methane ligands as indicated in Scheme 1.

Based on Scheme 1, a kinetic model can be constructed which uses the parameters k_{add} , k_{diss} , and k_{ex} . While kinetic isotope effects associated with H and D atom transfer or the losses of (labeled) methane might also play a role (*e. g.* $KIE_{ex} = k_{ex,H}/k_{ex,D}$), incorporation of other parameters was not pursued any further, because consideration of k_{add} , k_{diss} , and k_{ex} already suffices to reproduce the experimental data within the error margins, such that introduction of further parameters would not be justified. In this context it is noted, however, that the KIE s cannot be very large because the occurrence of extensive H/D exchange is obvious from the mere inspection of the data in Table 1. Further, several reactions of related Pt-containing cations have not revealed the operation of particularly large KIE s for the C–H(D) bond activation of methane in the gas phase [13, 25, 26]. The resulting kinetic model can be tested by application of the boundary conditions. Thus, for $k_{ex} \gg k_{diss}$ the statistical distribution is obtained, and for $k_{ex} \ll k_{diss}$ the product ion $[(CD_3)Pt(L)]^+$ is predicted to be formed almost exclusively. Another boundary condition evolving from the experiments is that k_{add} must be much smaller than k_{diss} , because otherwise the formation of a significant amount of adduct complexes would be implied, which is not the case in experiment. Further,

Table 2. Kinetic parameters^a for the H/D exchange between [(CH₃)Pt(L)]⁺ and CD₄ derived from kinetic modeling.

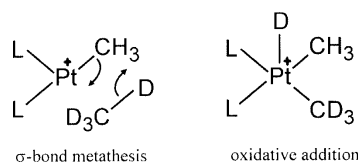
	$k_{\text{rel}}^{\text{b}}$	$k_{\text{ex}}/k_{\text{add}}^{\text{c}}$	$k_{\text{diss}}/k_{\text{add}}^{\text{d}}$	$k_{\text{ex}}/k_{\text{diss}}$
[(CH ₃)Pt(py)] ⁺	1.00	400 ± 50	80 ± 10	5 ± 1
[(CH ₃)Pt(bipy)] ⁺	0.19 ± 0.06	2500 ± 200	100 ± 10	25 ± 5
[(CH ₃)Pt(phen)] ⁺	0.17 ± 0.05	400 ± 50	80 ± 10	5 ± 1

a) See also text for further details; b) overall rate constants relative to the reaction for L = py; c) rate constant of the H/D exchange within the adduct complex relative to the rate constant for adduct formation; d) rate constant for dissociation of the adduct complex relative to the rate constant for adduct formation.

the kinetic modeling also allows the inclusion of secondary exchange reactions of the primary product ions with the neutral CD₄ present in a large excess, thereby permitting the determination of the intrinsic kinetic parameters associated with single-collision conditions.

Table 2 summarizes the kinetic parameters derived from the data given in Table 1. The first implication of these findings is that the pyridine complex reacts about five times faster compared to the complexes of bipy and phen, which can be attributed to the fact that the monodentate pyridine leaves the metal cation more reactive compared to the bidentate bipy and phen ligands. With regard to the intrinsic parameters of the H/D exchange processes, the behavior of all three complexes is qualitatively similar in that (i) k_{ex} as well as k_{diss} are both much larger than k_{add} and (ii) k_{ex} exceeds k_{diss} as already implied upon inspection of the raw data in Table 1. However, k_{ex} and k_{diss} are of the same order of magnitude for [(CH₃)Pt(py)]⁺ and [(CH₃)Pt(phen)]⁺, which highlights the necessity of the kinetic modeling. While the difference of k_{ex} and k_{diss} is larger in the case of [(CH₃)Pt(bipy)]⁺, the product distribution is still far from statistical. The reason why H/D exchange is incomplete even for a value of $k_{\text{ex}}/k_{\text{diss}} = 25$ lies in the large difference between k_{add} and k_{diss} , such that the amount of the primary exchange product [(CD₃)Pt(L)]⁺ exceeds that which would be predicted for statistical H/D exchange. Interestingly, H/D exchange is most pronounced in the case of the bipyridine complex. Although a more profound insight would require much more detailed studies, and preferentially also the inclusion of quantum-chemical treatments, as a plausible explanation we propose that the higher flexibility of the bipy ligand in comparison to phen [27] leads to an increased lifetime of the intermediate methane complexes, which would result in an increased $k_{\text{ex}}/k_{\text{diss}}$ ratio and thus enhance the amount of H/D exchange.

Despite the insight into the relative rate constants achieved this way, the present experimental findings



Scheme 2. Key structures involved in the H/D exchange of methane *via* σ bond metathesis and oxidative addition, respectively.

do not permit any conclusion with regard to the actual reaction mechanism. Specifically, the cleavage of the C–H bond in the methane ligand coupled with the formation of a new C–H bond to the methyl carbon atom can occur *via* two fundamentally different routes: either σ bond metathesis in which bond cleavage and bond formation occur simultaneously without any change of the oxidation state of the metal center, or oxidative addition, which leads to a formal Pt(IV) intermediate and thus a stepwise sequence for bond cleavage and bond formation (Scheme 2).

Last but not least, let us briefly return to the absence of any H/D exchange of [(CH₃)Pt(py)₂]⁺ in the presence of CD₄. Formally, [(CH₃)Pt(py)₂]⁺ might be considered as a close congener of [(CH₃)Pt(bipy)]⁺ and a similar reactivity might thus be expected. Obviously, however, the absence of a direct covalent linkage between the two nitrogen ligands leads to a different geometry of the cluster in the case of [(CH₃)Pt(py)₂]⁺ when compared to [(CH₃)Pt(bipy)]⁺, such that the platinum center is not anymore capable of activating the incoming methane molecule.

Conclusions

Electrospray mass spectrometry offers a simple way for the generation of gaseous [(CH₃)Pt(L)]⁺ complexes with the three representative nitrogen ligands L = pyridine, 2,2'-bipyridine, and 1,10-phenanthroline. All three [(CH₃)Pt(L)]⁺ complexes are capable of activating methane in thermal ion/molecule reactions, as demonstrated by the occurrence of H/D exchange when using CD₄. Of these complexes, [(CH₃)Pt(py)]⁺ with the monodentate pyridine as a ligand is about five times more reactive than the complexes with the bidentate nitrogen donors bipy and phen, which can be attributed to the lower coordination of the platinum center in [(CH₃)Pt(py)]⁺. Interestingly, however, the related complex [(CH₃)Pt(py)₂]⁺ is unable to activate methane at thermal conditions, although its coordination may formally be considered similar to the complexes of bipyridine and phenanthroline.

Acknowledgement

This work was part of B. Butschke's laboratory course "Organische Chemie II" at the Technische Universität Berlin.

Financial support by the Deutsche Forschungsgemeinschaft (SFB 546) and the Fonds der Chemischen Industrie is gratefully acknowledged.

-
- [1] A. E. Shilov, *Activation of saturated hydrocarbons by transition metal complexes*, Reidel, Dordrecht, **1984**.
- [2] R. A. Periana, D. J. Taube, S. Gamble, H. Taube, T. Sato, H. Fuji, *Science* **1998**, *280*, 560.
- [3] J. A. Labinger, *J. Mol. Catal.* **2004**, *220*, 27.
- [4] M. Lersch, M. Tilset, *Chem. Rev.* **2005**, *105*, 2471.
- [5] H. Schwarz, D. Schröder, *Pure Appl. Chem.* **2000**, *72*, 2319.7.
- [6] J. A. Labinger, J. E. Bercaw, M. Tilset, *Organometallics* **2006**, *25*, 805.
- [7] G. Gerdes, P. Chen, *Organometallics* **2006**, *25*, 809.
- [8] L. Johansson, M. Tilset, J. A. Labinger, J. E. Bercaw, *J. Am. Chem. Soc.* **2000**, *122*, 10846.
- [9] G. Gerdes, P. Chen, *Organometallics* **2003**, *22*, 2217.
- [10] J. B. Fenn, *Angew. Chem. Int. Ed.* **2003**, *42*, 3871.
- [11] D. Schröder, T. Weiske, H. Schwarz, *Int. J. Mass Spectrom.* **2002**, *219*, 729.
- [12] Calculated using the Chemputer made by M. Winter, University of Sheffield, see: <http://winter.group.shef.ac.uk/chemputer/>.
- [13] D. Schröder, H. Schwarz, *Can. J. Chem.* **2005**, *83*, 1936.
- [14] See also: D. Schröder, J. Loos, H. Schwarz, R. Thissen, O. Dutuit, *Inorg. Chem.* **2001**, *40*, 3161.
- [15] D. Schröder, H. Schwarz, S. Schenk, E. Anders, *Angew. Chem. Int. Ed.* **2003**, *42*, 5087.
- [16] J. Roithová, J. Hrušák, D. Schröder, H. Schwarz, *Inorg. Chim. Acta* **2005**, *358*, 4287.
- [17] D. Schröder, M. Engeser, H. Schwarz, E. C. E. Rosenthal, J. Döbler, J. Sauer, *Inorg. Chem.* **2006**, *45*, 6235.
- [18] D. Schröder, J. Roithová, *Angew. Chem. Int. Ed.* **2006**, *45*, 5705.
- [19] D. Schröder, J. Roithová, H. Schwarz, *Int. J. Mass Spectrom.* **2006**, *254*, 197.
- [20] C. Trage, D. Schröder, H. Schwarz, *Chem. Eur. J.* **2005**, *11*, 618.
- [21] J. Loos, D. Schröder, W. Zummack, H. Schwarz, R. Thissen, O. Dutuit, *Int. J. Mass Spectrom.* **2002**, *214*, 105.
- [22] C. Trage, D. Schröder, H. Schwarz, *Organometallics* **2003**, *22*, 693 (addendum **2003**, *22*, 1348).
- [23] J. Loos, D. Schröder, H. Schwarz, *J. Org. Chem.* **2005**, *70*, 1073.
- [24] J. Loos, D. Schröder, H. Schwarz, R. Thissen, O. Dutuit, *Int. J. Mass Spectrom.* **2005**, *240*, 121.
- [25] R. Wesendrup, D. Schröder, H. Schwarz, *Angew. Chem. Int. Ed. Engl.* **1994**, *33*, 1174.
- [26] K. Koszinowski, D. Schröder, H. Schwarz, *Organometallics* **2003**, *22*, 3809.
- [27] N. G. Tsierkezos, M. Diefenbach, J. Roithová, D. Schröder, H. Schwarz, *Inorg. Chem.* **2005**, *44*, 4969.